

2006, *110,* 16162–16164 Published on Web 08/03/2006

Identification of CO Adsorption Sites in Supported Pt Catalysts Using High-Energy-Resolution Fluorescence Detection X-ray Spectroscopy

Olga V. Safonova,† Moniek Tromp,*,‡ Jeroen A. van Bokhoven,*,§ Frank M. F. de Groot, John Evans,‡,⊥ and Pieter Glatzel†

European Synchrotron Radiation Facility, 6 rue Jules Horowitz, 38043 Grenoble, France, School of Chemistry, University of Southampton, Southampton, SO17 1BJ, United Kingdom, Institute for Chemical and Bioengineering, ETH Zurich, 8093 Zurich, Switzerland, Department of Inorganic Chemistry and Catalysis, Sorbonnelaan 16, 3584 CA, Utrecht, The Netherlands, and Diamond Light Source, Chilton, Didcot, OX11 0QX, United Kingdom

Received: June 2, 2006; In Final Form: July 6, 2006

High-energy-resolution fluorescence detection (HERFD) X-ray spectroscopy is presented as a new tool for the identification of the bonding sites of reactants in supported metal catalysts. The type of adsorption site of CO on an alumina-supported platinum catalyst and the orbitals involved in the bonding are identified. Because X-ray absorption spectroscopy (XAS) is element-specific and can be used under high pressures and temperatures, in situ HERFD XAS can be applied to a swathe of catalytic systems, including alloys.

Metal nanoparticles are used in many catalytic processes such as selective and total oxidation and hydrogenation reactions. The reactivity of nanoparticles depends greatly on their size, morphology, and the nature of the support. Understanding the correlation between the structure of the active sites and the performance of the catalytic system is extremely important for the design of better catalysts to increase conversion and selectivity to a desired reaction product. However, no characterization technique is capable of providing all information on the structures of catalytic sites under reaction conditions on real catalyst particles. Here, we present high-energy-resolution fluorescence detection (HERFD) X-ray spectroscopy as a new tool for the identification of the bonding sites of reactants in supported metal catalysts. The types of adsorption sites of CO on platinum on alumina catalyst and the orbitals involved in the bonding are identified.

The geometry of the CO adsorption site on perfect and stepped single crystal surfaces has been intensively studied by vibration spectroscopy, low-energy electron diffraction (LEED), and scanning tunneling microscopy. Three main CO adsorption configurations on Pt surfaces were identified: atop (one-fold), bridged (two-fold), and face bridging (three-fold). The overall conclusion is that CO prefers coordination to a single Pt atom at the lowest coverage and the atop-bridge combination at high coverage. The picture is similar for oxide-supported platinum nanoparticles, however, the support composition, its acidity, and pore curvature influence the CO adsorption geometry. The support composition geometry.

The sensitivity of the near-edge structure of X-ray absorption spectra (XANES) of metal nanoparticles to the presence of

[⊥] Diamond Light Source.

adsorbed molecules and the correlation between the shapes of Pt L edges and the geometry of the hydrogen and oxygen adsorption sites in supported Pt nanoparticles have been reported.¹⁰ According to the optical dipole selection rule, L_{2,3} X-ray absorption spectroscopy probes predominantly the dprojected empty density of states (DOS). The intensity of the first feature in the L₃ edge spectrum (the whiteline) probes the number of holes in the d-band. Changes in the XANES after molecular adsorption originate from orbital rehybridization, charge transfer, metal-absorbate scattering, and differences in metal-metal scattering. Intrinsic broadening of the experimental spectra occurs because of the finite lifetime of the core hole, rendering the experimental XAS spectra much broader than the actual DOS. For example, the lifetime broadening of the Pt 2p_{3/2} (L₃) core level measured by XPS is equal to 5.3 eV. 11a To detect subtle variations in the XANES region, detection of XAS spectra with higher resolution is required. The first attempts to overcome this fundamental limitation were undertaken by Hämäläinen, 11b who observed the spectral sharpening of a Dy XANES spectrum by monitoring only the Dy $L\alpha_1$ fluorescence with an energy resolution better than the core hole lifetime broadening. De Groot and co-workers measured the Pt L edges by monitoring $L\beta$ fluorescence lines with 2 eV resolution¹² and showed that HERFD spectra have a much better resolved fine structure compared to the XANES spectra measured in transmission mode. We have recently shown this to be similar for Au L₃ HERFD XANES (monitoring $L\alpha_1$), providing insights in the activation of oxygen and its reaction with CO over an Au/Al₂O₃ catalyst.13

Here, we present the first application of HERFD X-ray absorption spectroscopy as a probe of the bonding sites of adsorbed molecules on the surface of supported nanoparticles. The details on the synthesis of the supported Pt nanoparticles, the in situ reactor, the experimental conditions, and the theoretical calculations are given in the Supporting Information.

^{*} To whom correspondence should be addressed. E-mail: m.tromp@soton.ac.uk; J. A.vanBokhoven@chem.ethz.ch.

[†] European Synchrotron Radiation Facility.

University of Southampton.

[§] Institute for Chemical and Bioengineering.

Department of Inorganic Chemistry and Catalysis.

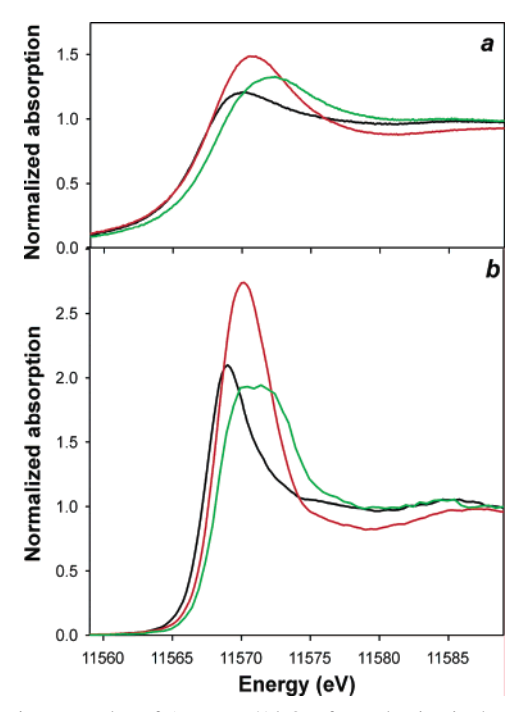


Figure 1. Pt L₃ edge of 5 wt % Pt/Al₂O₃ after reduction in the presence of different atmospheres: He (black), He(O2) (red), and 1% CO/He (green) measured using total fluorescence detection (a) and HERFD XAS spectroscopy (b).

The experiments were performed at the high brilliance XAFS-XES beamline ID26, at the European Synchrotron Radiation Facility (ESRF) in Grenoble, France. The incident energy was selected by means of a pair of Si(220) crystals with an energy bandwidth of 0.7 eV. The HERFD was performed with a horizontal plane Rowland circle spectrometer tuned to the Pt Lα₁ (9442 eV) fluorescence line. An energy bandwidth of 1.0 eV in the emission detection was achieved using the (660) Bragg reflection of one spherically bent Ge wafer. An avalanche photodiode (APD) was used as a detector. A Canberra silicon photodiode was mounted to measure the total fluorescence simultaneously.

Figure 1 compares the near-edge structure of the Pt L₃ edge of 5 wt % Pt/Al₂O₃ measured under different conditions using total fluorescence detection and HERFD. The sample was reduced in H₂ at 473 K. The H₂ was subsequently removed in He at 473 K. The XANES spectra, see Figure 1, were recorded in situ under steady-state conditions in, respectively, He, He with traces of O2 (He(O2)), and in 1% CO/He at 298 K. A change in atmosphere leads to variations in the shape of the whiteline for both detection techniques. However, by the use of HERFD spectroscopy, these variations are more pronounced and better resolved. The spectrum of Pt/Al₂O₃ after reduction shows the typical whiteline of reduced platinum particles. The intensity in the HERFD spectra, Figure 1b, is higher and structure becomes visible at 11576 eV. In both the total fluorescence detection and HERFD (parts a and b of Figure 1, respectively), the spectrum under He(O₂) shows increased whiteline intensity and a loss of intensity at 10-20 eV above the absorption edge, which is indicative of partial particle oxidation. Under a 1% CO/He atmosphere, the spectrum shows an energy shift and enhanced intensity in the whiteline that is broadened at the high-energy side. The HERFD data show the enhanced whiteline and reveal a double feature.

To identify the bonding sites of CO, we performed calculations of the Pt L₃-edge spectra using the FEFF8.2 code. ¹⁴ Four different clusters were considered as models for the adsorption

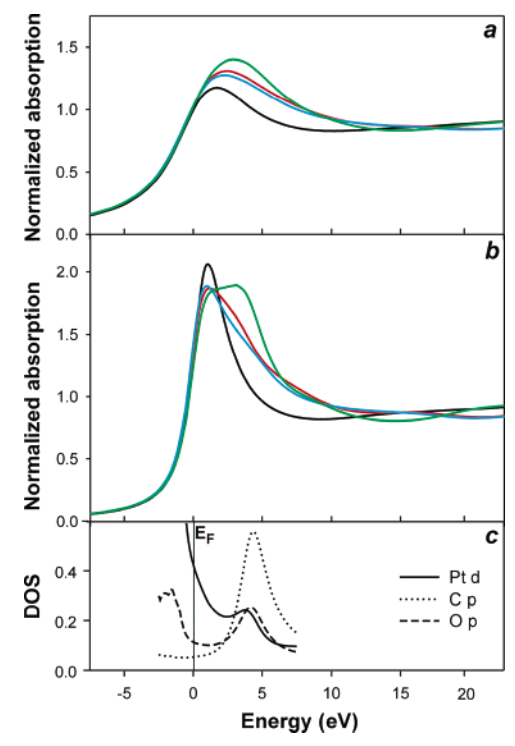


Figure 2. Theoretical (FEFF8.2) Pt L₃ edge of the Pt₆ cluster (black) and the Pt₆-CO clusters for CO atop (green), bridged (red), and face bridging (blue) with broadening (a) natural and (b) reduced by -1.6eV; (c) the d-DOS for Pt and p-DOS for C and O calculated for a Pt₆-CO atop cluster.

sites: Pt₆, ^{10b} Pt₆-CO atop, Pt₆-CO bridged, and Pt₆-CO face bridging. Diagrams of the clusters are given in the Supporting Information. The lifetime broadenings of L₃ and M₅ levels tabulated in the FEFF8.2 code¹⁴ are equal to 5.2 and 2.4 eV, respectively. According to the equation given in ref 12, the broadening due to the core hole lifetimes is equal to 2.2 eV in the HERFD spectra. The HERFD broadening (Lorentzian) is convoluted with the experimental broadening (Gaussian) and the width of Pt whiteline in the HERFD experiment should thus be close to 2.9 eV, which is similar to the value observed in the experiment. The line broadening in the FEFF calculations is given by the core hole lifetimes as well as the imaginary part of the self-energy.¹⁴ The line broadening can be reduced by using the EXCHANGE card in the FEFF input. The best agreement with experiment was achieved by using a value of vio = -1.6 eV.

Parts a and b of Figure 2 show the theoretical spectra of the bare and CO-containing platinum clusters without and with spectral sharpening, respectively. It was pointed out by Carra et al. 15 that strong electron-electron interactions (multiplet effects) can render a HERFD spectrum different from an absorption spectrum. In particular, additional spectral features might appear or disappear that are not due to an absorption process. 16 This effect is strong for localized orbitals such as valence band 3d or 4f levels, and even in those cases, these effects are only visible if the overall resolution is below 1.0 eV.¹⁷ We did not observe any multiplet effects in the 2p to 5d transition (white line) and thus conclude that a HERFD spectrum gives a very good approximation of an absorption scan. Furthermore, the FEFF calculations accurately reproduce all HERFD spectral features.

The shape of the XANES in the spectrum of the reduced Pt₆ cluster is similar to the experimental one with both detection techniques (Figures 1 and 2). The high-energy-resolution FEFF

simulation (Figure 2b) of atop adsorbed CO on Pt shows the double feature in the whiteline, which is absent in the simulations of the other configurations. These calculations indicate that in 1% CO/He atmosphere, the predominant geometry of the CO adsorption site on Pt nanoparticles is atop rather than bridged or face bridging. This distinction is much more pronounced in the HERFD spectrum. The DOS calculated for the Pt₆-CO atop cluster with FEFF are given in Figure 2c. They show that d-orbitals on the metal are overlapping with the $2\pi^*$ orbitals of the C and O atoms, forming an antibonding state above the Fermi level. This is reflected in the second feature of the whiteline in the HERFD spectrum of Pt/Al₂O₃ in 1% CO/ He (Figure 1b). The transition has a substantial metal-to-ligand charge-transfer character. For Pt₆-CO bridged and hollow sites, this component is weaker because the spatial distribution of the orbitals is less favorable for mixing.

In IR spectroscopy, probing the adsorbing molecule, variations in the stretching vibration of CO are related to the adsorption sites. In the HERFD XAS experiment, we can directly probe the structures of the adsorption sites and the DOS that are involved in the bonding. Therefore, HERFD and the vibrational spectroscopies provide complementary information and can be applied simultaneously. Because XAS is element-specific and can be used under high pressures and temperatures, in situ HERFD can be applied to a swathe of catalytic systems, including alloys.

Acknowledgment. The authors acknowledge ESRF for provision of facilities at ID26 and ID24 (mass spectrometer) and financial support (EPSRC to M.T. and the Swiss National Science Foundation to J.A.vB.). They also acknowledge Dr. M. Sikora for help in the preparation of the HERFD experiment.

Supporting Information Available: Details on the synthesis of alumina-supported Pt nanoparticles, the in situ reactor, experimental conditions and theoretical calculations, and XAFS data under dynamic conditions. This material is available free of charge via the Internet at http://pubs.acs.org.

References and Notes

- (1) (a) Eischens, R. P.; Plishkin, W. A. Adv. Catal. 1958, 10, 1. (b) Eischens, R. P.; Francis, S. A.; Plishkin, W. A. J. Phys. Chem. 1956, 60, 194. (c) Hollins, P. Surf. Sci. Rep. 1992, 16, 51. (d) Schweizer, E.; Persson, B. N. J.; Tushaus, M.; Hoge, D.; Bradshaw, A. M. Surf. Sci. 1989, 213, 49. (e) Hayden, B. E.; Kretschmar, K.; Bradshaw, A. M.; Greenler, R. G. Surf. Sci. 1985, 149, 394.
- (2) (a) Ogletree, D. F.; van Hove, M. A.; Somorjai, G. A. Surf. Sci. 1986, 173, 351. (b) Blackman, G. S.; et al. Phys. Rev. Lett. 1988, 61, 2352.
 (3) (a) Bocquet, M. L.; Sautet, Ph. Surf. Sci. 1996, 360, 128. (b) Pedersen, M. O.; Bocquet, M. L.; Sautet, Ph.; Laegsgaard, E.; Stensgaard, I.; Besenbacher, F. Chem. Phys. Lett. 1999, 299, 403.
- (4) Feibelman, P. J.; Hammer, B.; Nørskov, J. K.; Wagner, F.; Scheffler, M.; Stumpf, R.; Watwe, R.; Dumesic, J. J. Phys. Chem. B. 2001, 105, 4018.
 (5) Mojet, B. L.; Miller, J. T.; Koningsberger, D. C. J. Phys. Chem. B 1999, 103, 2724.
- (6) (a) Barth, R.; Pitchai, R.; Anderson, R. L.; Verykios, X. E. J. Catal.
 1989, 116, 61. (b) Barth, R.; Ramachandran, A. J. Catal.
 1990, 125, 467.
 (7) Gandao, Z.; Coq, B.; de Menorval, L. C.; Tichit, D. Appl. Catal. A
 1996, 147, 395.
- (8) Fiddy, S. G.; Newton, M. A.; Campbell, T.; Dent, A. J.; Harvey, I.; Salvini, G.; Turin, S.; Evans, J. Phys. Chem. Chem. Phys. 2002, 4, 827. (9) Visser, T.; Nijhuis, T. A.; van der Eerden, A. M. J.; Jenken, K.; Ji, Y.; Bras, W.; Nikitenko, S.; Ikeda, Y.; Lepage, M.; Weckhuysen, B. M. J. Phys. Chem. B 2005, 109, 3822.
- (10) (a) Oudenhuijzen, M. K.; van Bokhoven, J. A.; Miller, J. T.; Ramaker, D. E.; Koningsberger, D. C. *J. Am. Chem. Soc.* **2005**, *127*, 1530. (b) Ramaker, D. E.; Teliska, M.; Zhang, Y.; Stakheev, A. Yu.; Koningsberger, D. C. *Phys. Chem. Chem. Phys.* **2003**, *5*, 4492. (c) Ankudinov, A. L.; Rehr, J. J.; Low, J. J.; Bare, S. R. *Top. Catal.* **2002**, *18*, 3.
- (11) (a) Fuggle, J. C.; Inglesfield, J. E. *Unoccupied Electronic States*; Springer-Verlag: Berlin, 1992. (b) Hämäläinen, K.; Siddons, D. P.; Hastings, J. B.; Berman, L. E. *Phys. Rev. Lett.* **1991**, *67*, 2850.
- (12) de Groot, F. M. F.; Krish, K. H.; Vogel, J. Phys. Rev. B. 2002, 66, 195112.
- (13) van Bokhoven, J. A.; Louis, C.; Miller, J. T.; Tromp, M.; Safonova, O. V.; Glatzel, P. *Angew. Chem., Int. Ed.* **2006**, *45* (28), 4651; *Angew. Chem.* **2006**, *118*, 4767.
- (14) (a) Ankudinov, A. L.; Ravel, B.; Rehr, J. J.; Conradson, S. D. *Phys. Rev. B* **1998**, *58*, 998. (b) Ankudinov, A. L.; Bouldin, C.; Rehr, J. J.; Sims, J.; Hung, H. *Phys. Rev. B* **2002**, *65*, 104107.
- (15) Carra, P.; Fabrizio, M.; Thole, B. T. Phys. Rev. Lett. 1995, 74, 3700.
 - (16) Glatzel, P.; Bergmann, U. Coord. Chem. Rev. 2005, 249, 65.
- (17) de Groot, F. M. F.; Glatzel, P.; Bergmann, U.; van Aken, P. A.; Barrea, R. A.; Klemme, S.; Havecker, M.; Knop-Gericke, A.; Heijboer, W. M.; Weckhuysen, B. M. *J. Phys. Chem. B* **2005**, *109*, 20751.